



University of
New Haven

University of New Haven
Digital Commons @ New Haven

Civil Engineering Faculty Publications

Civil Engineering

2-3-2018

Stabilization of Lead (Pb) and Zinc (Zn) in Contaminated Rice Paddy Soil Using Starfish: A Preliminary Study

Deok Hyun Moon
Chosun University

Inseong Hwang
Pusan National University


Agamemnon Koutsospyros
University of New Haven, akoutsospyros@newhaven.edu

Kyung Hoon Cheong
Chosun University

Yong Sik Ok
Korea University

See next page for additional authors

Follow this and additional works at: <https://digitalcommons.newhaven.edu/civilengineering-facpubs>

 Part of the [Civil Engineering Commons](#), and the [Ecology and Evolutionary Biology Commons](#)

Publisher Citation

Moon, D. H., Hwang, I., Koutsospyros, A., Cheong, K. H., Ok, Y. S., Ji, W. H., & Park, J. (2018). Stabilization of lead (Pb) and zinc (Zn) in contaminated rice paddy soil using starfish: A preliminary study. *Chemosphere*. doi:10.1016/j.chemosphere.2018.01.090

Comments

This is the authors' accepted version of the article published in *Chemosphere*. The final publication is available at Springer via <http://doi:10.1016/j.chemosphere.2018.01.090>.

Authors

Deok Hyun Moon, Inseong Hwang, Agamemnon Koutsospyros, Kyung Hoon Cheong, Yong Sik Ok, Won Hyun Ji, and Jeong Hun Park

31 **Abstract**

32

33 Lead (Pb) and zinc (Zn) contaminated rice paddy soil was stabilized using natural (NSF) and calcined starfish (CSF).
34 Contaminated soil was treated with NSF in the range of 0-10 wt.% and CSF in the range of 0-5 wt.% and cured for 28 days.
35 Toxicity characteristic leaching procedure (TCLP) test was used to evaluate effectiveness of starfish treatment. Scanning
36 electron microscopy-energy dispersive X-ray spectroscopy (SEM-EDX) analyses were conducted to investigate the
37 mechanism responsible for effective immobilization of Pb and Zn. Experimental results suggest that NSF and CSF
38 treatments effectively immobilize Pb and Zn in treated rice paddy soil. TCLP levels for Pb and Zn were reduced with
39 increasing NSF and CSF dosage. Comparison of the two treatment methods reveals that CSF treatment is more effective
40 than NSF treatment. Leachability of the two metals is reduced approximately 58% for Pb and 51% for Zn, upon 10% NSF
41 treatments. More pronounced leachability reductions, 93% for Pb and 76% for Zn, are achieved upon treatment with 5 wt.%
42 CSF. Sequential extraction results reveal that NSF and CSF treatments of contaminated soil generated decrease in
43 exchangeable/weak acid Pb and Zn soluble fractions, and increase of residual Pb and Zn fractions. Results for the SEM-
44 EDX sample treated with 5 wt.% CSF indicate that effective Pb and Zn immobilization is most probably associated
45 with calcium silicate hydrates (CSHs) and calcium aluminum hydrates (CAHs).

46

47 **Keywords:** Immobilization, Heavy metals, Starfish, Sequential extraction, TCLP

48

49

50

51

52

53

54

55

56

57

58

59

60

61 **Introduction**

62

63 Heavy metal contamination in rice paddy soil is a major concern because of its toxicity to human health. Pb and Zn are
64 common heavy metals released from abandoned or closed mines in the Republic of Korea that cause rice paddy soil
65 contamination. There are approximately 2,600 abandoned mines in the Republic of Korea and among them 1,301 mines
66 are associated with serious heavy metal release problems (Mine Reclamation Corp., 2014). Stabilization offers a viable
67 alternative for remediation of Pb and Zn contaminated rice paddy soils.

68 Traditionally, stabilization technologies have relied on two main sources of stabilizing agents, chemical products
69 (hydrated lime, quicklime) (Jing, et al., 2004; Moon, et al., 2004) and industrial by-products (Portland cement, cement kiln
70 dust, fly ash, etc.) (Wang and Vipulanandan, 1996; Li, et al., 2001; Dermatas and Meng, 2003; Moon and Dermatas, 2007;
71 Moon, et al., 2008), for effective immobilization of heavy metals. Recently, attention has shifted towards low-cost, more
72 sustainable alternatives that use natural waste materials (i.e. waste oyster shells) as stabilizing agents for immobilization of
73 heavy metals in contaminated soils (Moon, et al., 2011; Moon, et al., 2013; Moon, et al., 2015).

74 Consistent to this viewpoint, this study considers use of starfish as a stabilizing agent for remediation of Pb and Zn
75 contaminated rice paddy soil. In recent years, starfish have been recognized as a major problem leading to degradation of
76 natural marine ecosystems. Starfish exhibit a high reproductive rate capable of laying 2-3 million eggs at a time.
77 Additionally, starfish are known bottom feeders, capable of consuming large amounts of various benthic invertebrate
78 organisms including ear shells, sea cucumbers, short-necked clams, shellfish, sea urchins, etc. An individual starfish
79 organism usually consumes approximately 10 kg/yr of the above-mentioned sea organisms. Even though the triton shell is
80 a natural predator of starfish, its population is limited and the only viable alternative for controlling outbreaks of these
81 invasive species is capturing great numbers of starfish, often exercised by oystermen. However, marketing and recycling
82 options for captured starfish have been scarce. Beneficial uses reported in literature include applications of starfish as
83 a fertilizer (Park, 2003), or as additive for heavy metal removal (Hong, et al., 2011). Alternatively, starfish, a
84 feedstock of high calcium content enhanced with various other minor elements (i.e. Mg, P, K, Zn, etc.), has recently
85 been used as an amendment for acidic soil remediation (Lebrato, et al., 2013; Moon, et al., 2014).

86 The calcination process, achieved at high temperatures (900°C for 2 hours), converts calcite (CaCO_3), the main
87 inorganic constituent of starfish, into quicklime (CaO). Previously, calcination at 700°C and 900°C was applied
88 to produce calcined starfish for amelioration of acidic soil (Moon, et al., 2014). Reportedly, heavy metal
89 immobilization with calcite and quicklime is achieved by formation of pozzolanic reaction products such as calcium silicate
90 hydrates (CSHs) or calcium aluminum hydrates (CAHs) (Rose, et al., 2000; Dermatas and Meng, 2003; Moon, et al.,

91 2006). Therefore, it may be postulated that Pb and Zn immobilization in contaminated soil using natural state or calcined
92 starfish can be attained based on formation of pozzolanic reaction products.

93 The objective of this study is to evaluate feasibility of beneficially using starfish for immobilization of Pb and
94 Zn in contaminated soil. The effectiveness of the immobilization process was evaluated using the Toxicity
95 characteristic leaching procedure (TCLP) test (USEPA, 1992). Scanning electron microscopy-energy dispersive X-
96 ray spectroscopy (SEM-EDX) analyses were conducted to investigate the mechanism responsible for effective Pb
97 and Zn immobilization in contaminated soil treated with starfish as a stabilizing agent.

98

99 **Experimental methodology**

100

101 Contaminated soil collection

102

103 Lead (Pb) and zinc (Zn) contaminated rice paddy soil was collected from a farmland near an abandoned gold mine at
104 Jeong Eup City, Republic of Korea. This mine, active since the early 1900s, operated for extraction of gold, silver,
105 copper, and zinc until its closure in 1992. Contaminated soil was sampled at a depth of 0-30 cm from soil surface.
106 Collected soil sample was air-dried and sieved through a United States standard #10 mesh (2mm) to exclude large
107 particles and attain homogeneity. Total concentrations of Pb and Zn in contaminated soil were 980 mg·kg⁻¹ and
108 890 mg·kg⁻¹, respectively. Contaminated soil was classified as sandy loam by a particle size analyzer (PSA) in
109 accordance with the United States Department of Agriculture (USDA). Soil pH was 7.22. Physicochemical and
110 mineralogical properties as well as total concentrations of Pb and Zn in contaminated soil are presented in Table
111 1. Bulk chemistry of the Pb and Zn contaminated soil measured by X-ray fluorescence (XRF, ZSX100e, Rigaku,
112 Japan) is presented in Table 2.

113

114 Stabilizing agents

115

116 The NSF used in this study were obtained from the seaside of Goseong-gun, Gyeongsangnam-do Province,
117 Republic of Korea. Initial NSF sample treatment included a multi-step rinsing using deionized (DI) water to
118 remove salty layer and other impurities. Additional treatment included air drying and grinding in a crushing mill
119 to achieve a fine, homogenized powder that passed through the United States standard #20 sieve (0.85 mm).
120 Calcination of NSF was accomplished in an electric furnace (J-FM3, JISICO, South Korea), operated at 900°C for

121 2 hours. Calcination process transformed calcite (CaCO_3), the main mineral NSF constituent, into quicklime (CaO)
122 (Fig. 1a-b). Major chemical composition for the NSF and CSF as determined by XRF are presented in Table 2.

123

124 Stabilization experiments

125

126 Heavy metal (Pb, Zn) contaminated soil samples were treated using 6 stabilizing-agent to soil mixing ratios for
127 NSF (0 wt.%, 2 wt.%, 4 wt.%, 6 wt.%, 8 wt.% and 10 wt.%) and CSF (0 wt.%, 1 wt.%, 2 wt.%, 3 wt.%, 4 wt.%
128 and 5 wt.%). The 0 wt.% mixing ratios for each stabilizing agent served as control treatments for benchmarking
129 purposes. Full hydration was ensured by water content of 20% in all treated samples. All treated samples were
130 cured for 28 days in a sealed plastic container at ambient temperature (20°C, 25% humidity). Sample designations
131 are shown in Table 3.

132

133 Analyses of chemical fractions

134

135 The sequential extraction procedure (SEP) developed by Tessier, et al. (1979) was used to investigate chemical
136 fractions of Pb and Zn in contaminated soil. This procedure allows identification of 5 distinct chemical fractions
137 designated as exchangeable (F1), weak acid soluble (F2), reducible (F3), oxidizable (F4) and residual (F5).
138 Samples of the most effective stabilization treatments (10 wt.% NSF and 5 wt.% CSF), along with control samples
139 were subjected to SEP analysis to assess differences in various Pb and Zn chemical fractions upon treatment.

140

141 X-ray powder diffraction (XRPD) analyses

142

143 X-ray powder diffraction (XRPD) analyses were conducted to investigate mineralogical changes. Sample pre-
144 treatment for XRPD analyses, included air-drying for 24 hours followed by pulverization into powder that cleared
145 the United States-standard #200 sieve (0.075 mm). A PANalytical X-ray diffraction (XRD) instrument (X'Pert
146 PRO MPD) was used for collection of step scanned X-ray diffraction patterns. A diffracted beam graphite-
147 monochromator with Cu radiation was used at 40 kV and 40 mA. The XRPD patterns were taken in the 2θ range
148 of 5-65° with a step size of 0.02° and a count time of 3 seconds per step. Jade software version 7.1 (MDI 2005)
149 and the PDF-2 reference database from the International Center for Diffraction Data database (ICDD, 2002) were
150 used for identification of mineral compositions.

151
152
153
154
155
156
157
158
159
160
161
162
163
164
165
166
167
168
169
170
171
172
173
174
175
176
177
178
179
180

SEM-EDX analyses

The treatment that produced the highest metal leachability reduction (5 wt.% CSF) was selected for SEM-EDX analysis. Initial sample pre-treatment for SEM-EDX analysis included air drying. Subsequently, sub-samples were placed on a double-sided carbon tape, coated with platinum (Pt) and were analyzed in a Hitachi S-4800 SEM instrument equipped with an ISIS 310 EDX system.

Physicochemical analyses

Soil pH values were obtained in accordance with the KST method (MOE 2002) at a liquid-to-solid (L: S) ratio of 5:1 l·kg⁻¹. Effectiveness of immobilization for Pb and Zn in the contaminated soil is evaluated by TCLP test in accordance with the United States EPA protocol (USEPA, 1992). Specifically, 3g of soil was mixed with 60 mL of TCLP solution and agitated in a TCLP tumbler for 18 hours. Since a TCLP regulatory limit for Zn is not currently in place, use of the Universal Treatment Standard (UTS) for Zn of 4.3 mg·l⁻¹, established in the LDR Rules and Regulations 1999 (USEPA, 1999), is warranted for comparison purposes. Use of the UTS standard for Zn has been documented in literature for a cement-based stabilization/solidification (S/S) study (Ruiz and Irabien, 2004) and for a cement, cement kiln dust and fly ash based S/S study (Moon, et al., 2010). Analytical determinations for total Pb and Zn were made using the following procedures: 1) aqua regia [0.7 ml of HNO₃ (65%, Merck) and 2.1 ml of HCl (37%, J.T. Baker)] addition to the soil sample (0.3 g) (MOE 2010); 2) mixture heating at 70°C for 2 hours and dilution with 7.2 ml of distilled water (MOE, 2010); 3) filtration of extracted solution through a 0.45-µm micropore filter; 4) analytical determination of filtrate soluble Pb and Zn concentrations using an inductively coupled plasma-optical emission spectrometer (ICP-OES, Optima 8300DV) (PerkinElmer, CT, USA). ICP-OES was used for determination of TCLP Pb and Zn concentrations. All ICP-OES determinations were conducted in duplicate or triplicate, and mean values were reported within 10% error. Three different quality control standards were used for every 20 samples analyzed to ensure QA/QC.

Results and discussion

Soil properties

181

182 Following 28 days of curing, the soil pH and organic contents were increased. The soil pHs upon 2-10 wt.% WOS
183 treatments ranged from 8.42 to 8.51. Moreover, the soil pHs upon 1-5 wt.% COS treatments ranged between 10.94
184 to 12.45. The soil pH increase was more pronounced upon COS treatment, due to high CaO content. The organic
185 contents upon WOS and COS treatment ranged from 3.77 to 3.94 and 3.21 and 3.47, respectively. The organic
186 content upon COS treatment was not notable due to the very low organic content of COS itself (0.87%).

187

188 XRPD analyses

189

190 X-ray powder diffraction (XRPD) analyses of the contaminated soil, presented in Table 1, reveals that quartz,
191 muscovite and albite are the main mineral phases. XRPD analyses revealed that the main phase in NSF is calcite
192 [(Ca, Mg) CO₃, PDF# 43-0697] mainly transformed into quicklime (CaO, PDF# 48-1467) in the CSF upon
193 calcination conducted at 900°C for 2 hours (Fig. 1).

194

195 Effectiveness of the stabilization treatment

196

197 TCLP Pb and Zn concentrations with the TCLP pH values of samples subjected to NSF and CSF treatment are
198 presented in Figs. 2 and 3. In NSF treated samples (Fig. 2a), TCLP Pb concentrations decreased with increasing
199 NSF content. Evidently all treatments at levels 4 wt.% NSF or higher produce Pb levels compliant to the TCLP
200 regulatory limit of 5 mg·l⁻¹. The lowest TCLP Pb concentration of 2.87 mg·l⁻¹, attained upon treatment with 10
201 wt.% NSF, represents a decrease of more than 58% in TCLP Pb concentration compared to the control sample. At
202 this point, it should be noted that NSF treatments at levels greater than 6 wt.% may not be warranted as they did
203 not produce commensurate reduction of TCLP Pb levels. It has been reported that a significant reduction (100%)
204 in TCLP Pb concentration was achieved in an 81 mg/L control sample, upon 10 wt.% NSF treatment (Lim, et al.,
205 2017). High reduction rate reported by Lim, et al. (2017) may depend on variability of starfish, soil characteristics
206 and the Pb form in the control and treated samples. Much like the TCLP Pb results, the TCLP Zn concentrations
207 (Fig. 2b) decreased with increasing NSF content. However, although all NSF treatments produced Zn level
208 reductions 50% or higher compared to the control, none was compliant to the UTS standard for Zn of 4.3 mg·l⁻¹.
209 The 10 wt.% NSF treatment produced marginally the lowest TCLP Zn concentration of 7.4 mg·l⁻¹. TCLP Zn level
210 reductions as high as 100% in the 6.5 mg/L control sample upon 10wt.% NSF treatment have been reported in

211 literature (Lim, et al., 2017). Higher reductions reported by Lim, et al. (2017), may be associated with variability
212 of starfish, soil characteristics, and the Zn form in control and treated samples.

213 In CSF treated samples (Fig. 3), reduction in TCLP Pb leachability (Fig. 3a) was more pronounced than that of
214 the NSF treated samples. 2 wt.% CSF was sufficient to ensure compliance with the TCLP regulatory limit of 5
215 $\text{mg}\cdot\text{l}^{-1}$. The lowest TCLP Pb concentration of $0.46 \text{ mg}\cdot\text{l}^{-1}$, attained upon 5 wt.% CSF treatment, represents a
216 reduction in TCLP Pb leachability of more than 93% compared to the control. A comparable TCLP Pb reduction
217 of 100% attained upon 5wt.% CSF treatment has been reported (Lim, et al., 2017). Similarly, the TCLP Zn
218 concentrations were significantly reduced upon CSF treatment compared to those obtained with NSF treatment.
219 This indicates that CSF treatment was more effective than NSF treatment and is evident by the lower TCLP Zn
220 concentrations for all treatment levels compared to those of NSF treatment. The lowest TCLP Zn concentration of
221 $3.61 \text{ mg}\cdot\text{l}^{-1}$ attained upon 5 wt.% CSF treatment complied with the UTS standard for Zn of $4.3 \text{ mg}\cdot\text{l}^{-1}$. It has been
222 reported that TCLP Zn reduction of 100% was observed upon 5 wt.% CSF treatment (Lim, et al., 2017). Based on
223 these results, it can be concluded that CSF treatment is highly effective in immobilizing Pb and Zn in contaminated
224 soils at relatively low dosage levels. This finding is corroborated by Lim, et al. (2017) that observed CSF treatment
225 was more effective than the NSF treatment. Based on results of SEM-EDX analyses, it can be postulated that
226 formation of pozzolanic reaction products, such as calcium silicate hydrates (CSHs) and calcium aluminum
227 hydrates (CAHs), are most likely responsible for Pb and Zn immobilization.

228

229 Sequential extraction results

230

231 Results of the SEP analysis are presented in Fig. 4. Since untreated and treated soil samples vary significantly in
232 terms of basic physicochemical properties and mineral composition, results of the SEP analysis of the soils are
233 used to theorize on relative binding strength of Pb and Zn. Upon 10 wt.% NSF treatments, exchangeable (F1) and
234 weak acid soluble (F2) fractions for Pb and Zn decreased. Reducible (F3), oxidizable (F4) and residual (F5)
235 fractions increased for Pb upon NSF treatment. In this case, Zn F4 and F5 fractions increased. Similarly, upon 5
236 wt.% CSF treatment, the F1 and F2 fractions for Pb and Zn significantly decreased. This reduction was more
237 pronounced as compared to the 10 wt.% NSF treatment. In the case of Pb, the F3, F4 and F5 fractions significantly
238 increased. It has been reported that in the case of Pb, decreases in F1 and F2 fractions were associated with increase
239 in the F3 fraction upon calcined oyster shell (COS) and coal mine drainage sludge (CMDS) treatment (Lee, et al.,
240 2013). This mixed treatment was like the CSF treatment since the main phase in COS was CaO. Lee, et al. (2013)

241 reported that changes in the fractions from F1, F2 and F3 supported the stabilization effect on Pb. In the case of
242 Zn, the F3 and F5 fractions increased but the F4 fraction was virtually similar. This suggested that reduction in the
243 F1 and F2 fractions and increase in the F3, F4 and F5 fractions for Pb are most probably associated with high
244 degree of stabilization achieved with NSF and CSF. In the case of Zn, reduction in F1 and F2 fractions and increase
245 in the F5 fraction was most probably linked to the high degree of stabilization achieved with NSF and CSF.

246

247 SEM-EDX results

248

249 SEM-EDX and mapping results for the 5 wt.% CSF treated sample are presented in Fig. 5. Pb and Zn were
250 identified by the SEM-EDX analysis (Fig. 5a). The Si content, displayed by the white color in the mapping results,
251 in all areas was very high. Even though low signals for Pb and Zn were detected due to low total contents, these
252 signals were strong in the targeted particle. Therefore, the elemental dot map results reveal that Pb and Zn
253 immobilization was most probably associated with Ca, Al, Si, and O due to the formation of pozzolanic reaction
254 products such as CSHs and CAHs (Fig. 5b). Support for this finding is well documented in literature. Reportedly,
255 Pb is immobilized within the CSH matrix by direct linkages at the end of silicate chains via Pb–O–Si bonds (Rose,
256 et al., 2000). Pb incorporation into the CSH structure has been reported as the key mechanism for effective Pb
257 immobilization using quicklime (Dermatas and Meng, 2003). In addition to previous research, specific types of
258 CSHs such as, $\text{CaH}_4\text{Si}_2\text{O}_7$ and $\text{Ca}_5\text{Si}_6\text{O}_{16}(\text{OH})_2$ were identified as phases strongly associated with effective Pb
259 immobilization upon quicklime treatment (Moon, et al., 2006). It has been reported that ettringite formation was
260 identified as responsible for Pb immobilization in a 10 wt.% CSF treated sample (Lim, et al., 2017). However,
261 ettringite was not observed in the 5 wt.% CSF treated sample because samples did not contain significant sulfate
262 levels. Therefore, ettringite may not be the phase linked to effective Pb immobilization. Ettringite,
263 $\text{C}_3\text{A}\cdot 3\text{CaSO}_4\cdot 32\text{H}_2\text{O}$ (Aft) or $\text{Ca}_6\text{Al}_2(\text{SO}_4)_3(\text{OH})_{12}\cdot 26\text{H}_2\text{O}$, is a key pozzolanic reaction mineral product (Moon, et
264 al., 2010) that can immobilize Pb inside of the ettringite crystal matrix by solid solution with Ca^{2+} (Gougar, et al.,
265 1996). Effective Zn immobilization may be achieved by a tricalcium silicate component (Bhatty, 1987) or CSHs
266 compounds. Zn incorporation into CSH structure has been reported to proceed either by replacement of Ca^{2+} or by
267 direct linkage to the end of silicate chains through Zn–O–Si bonds (Moulin, et al., 1999; Rose, et al., 2001).

268

269 **Conclusion**

270

271 In this study natural (NSF) and calcined starfish (CSF) were used to immobilize Pb and Zn in contaminated rice paddy
272 soil. The stabilization treatment results revealed that NSF and CSF treatments were effective in reducing TCLP
273 Pb and Zn leachability. The CSF treatment outperformed the NSF treatment. In order to comply with the TCLP
274 Pb regulatory limit of 5 mg·l⁻¹, 4 wt% NSF and 2 wt% CSF were required, respectively. In the case of Zn
275 immobilization, all NSF treatments failed and 5 wt% CSF was needed to pass the UTS standard for Zn at 4.3 mg·l⁻¹.
276 Chemical fraction analyses revealed that the effective Pb and Zn immobilization upon NSF and CSF treatment
277 was strongly associated with the residual phase. The SEM-EDX and mapping results indicated that pozzolanic
278 reaction products such as CSHs and CAHs may be the most probable compounds associated with effective Pb and
279 Zn immobilization.

280

281 **Acknowledgement**

282

283 This study was supported by the Korean Ministry of Environment as the GAIA (Geo-Advanced Innovative Action)
284 projects (No. 2015000550003 and No. 201503008).

285

286 **References**

287

288 Ball D.F., 1964. Loss-on-ignition as an estimate of organic matter and organic carbon in non-calcareous soil. J.
289 Soil Sci. 15, 84-92.

290 Bhatta, M.S.Y., 1987. Fixation of metallic ions in Portland cement. Superfund 87, 140-145.

291 Dermatas, D., Meng, X., 2003. Utilization of fly ash for stabilization/solidification of heavy metal contaminated
292 soils. Eng. Geol. 70, 377-394.

293 FitzPatrick, E.A., 1983. Soils: Their formation, classification and distribution. Longman Science & Technical,
294 London, p 353

295 Gougar, M.L.D., Scheetz, B.E., Roy, D.M., 1996. Ettringite and C-S-H Portland cement phases for waste ion
296 immobilization: A review. Waste Manage. 16(4), 295-303.

297 Hong, K.-S., Lee, H.-M., Bae, J.-S., Ha, M.-G., Jin, J.-S., Hong, T.-E., Kim, J.-P., Jeong, E.-D., 2011. Removal of
298 heavy metal ions by using calcium carbonate extracted from starfish treated by protease and amylase. J. Anal.
299 Sci. Technol. 2(2), 75-82.

300 ICDD, 2002. Powder diffraction file.PDF-2 database release, International Centre for Diffraction Data, Newtown
301 Square, Pennsylvania, USA.

302 Jing, C., Meng, X., Korfiatis, G.P., 2004. Lead leachability in stabilized/solidified soil samples evaluated with
303 different leaching tests. *J. Hazard. Mater.* B114, 101-110.

304 Lebrato, M., McClintock, J.B., Amsler, M.O., Ries, J.B., Egilsdottir, H., Lamare, M., Amsler, C.D., Challener,
305 R.C., Schram, J.B., Mah, C.L., Cuce, J., Baker, B.J., 2013. From the arctic to the antarctic: the major, minor,
306 and trace elemental composition of echinoderm skeletons. *Ecology* 94, 1434-1434.

307 Lee, K.-Y., Moon, D.H., Lee, S.-H., Kim, K.W., Cheong, K.-H., Park, J.-H., Ok, Y.S., Chang, Y.-Y., 2013.
308 Simultaneous stabilization of arsenic, lead, and copper in contaminated soil using mixed waste resources.
309 *Environ. Earth Sci.* 69, 1813-1820.

310 Li, X.D., Poon, C.S., Sun, H., Lo, I.M.C., Kirk, D.W., 2001. Heavy metal speciation and leaching behaviors in
311 cement based solidified/stabilized waste materials. *J. Hazard. Mater.* A 82, 215-230.

312 Lim, J.E., Sung, J.K., Sarkar, B., Wang, H., Hashimoto, Y., Tsang, D.C.W., Ok, Y.S., 2017. Impact of natural and
313 calcined starfish (*Asterina pectinifera*) on the stabilization of Pb, Zn and As in contaminated agricultural soil.
314 *Environ. Geochem. Health.* 39, 431-441.

315 MDI, 2005. Jade Version 7.1. Material's Data Inc., Livermore, California, USA.

316 Mine Reclamation Corp., 2014. 2013 Yearbook of MIRECO Statistics, p. 242 (in Korean).

317 Ministry of Environment (MOE), 2010. The Korean Standard Test (KST) methods for soils. Korean Ministry of
318 Environment, Gwachun, Kyunggi, p. 225 (in Korean).

319 Moon, D.H., Cheong, K.H., Khim, J., Grubb, D.G., Ko, I., 2011. Stabilization of Cu-contaminated army firing
320 range soils using waste oyster shells. *Environ. Geochem. Health* 33, 159-166.

321 Moon, D.H., Dermatas, D., 2007. Arsenic and lead release from fly ash stabilized/solidified soils under modified
322 semi-dynamic leaching conditions. *J. Hazard. Mater.* 141, 388-394.

323 Moon, D.H., Dermatas, D., Grubb, D.G., 2006. The effectiveness of quicklime-based stabilization/solidification
324 on lead (Pb) contaminated soils, In: *Environmental Geotechnics (5th ICEG)*, Thomas H.R. (ed.), Thomas
325 Telford Publishing, London, 1, 221-228.

326 Moon, D.H., Dermatas, D., Grubb, D.G., 2010. Release of arsenic (As) and lead (Pb) from quicklime-sulfate
327 stabilized/solidified soils under diffusion-controlled conditions. *Environ. Monit. Assess.* 169, 259-265.

328 Moon, D.H., Dermatas, D., Menounou, N., 2004. Arsenic immobilization by calcium-arsenic precipitates in lime
329 treated soils. *Sci. Total Environ.* 330, 171-185.

330 Moon, D.H., Park, J.-W., Cheong, K.H., Hyun, S., Koutsospyros, A., Park, J.-H., Ok, Y.S., 2013. Stabilization of
331 lead and copper contaminated firing range soil using calcined oyster shells and fly ash. *Environ. Geochem.*
332 *Health* 35, 705-714.

333 Moon, D.H., Yang, J.E., Cheong, K.H., Koutsospyros, A., Park, J.-H., Lim, K.J., Kim, S.C., Kim, R.-Y., Ok, Y.S.,
334 2014. Assessment of natural and calcined starfish for the amelioration of acidic soil. *Environ. Sci. Pollut. Res.*
335 21, 9931-9938.

336 Moon, D.H., Wazne, M., Cheong, K.H., Chang, Y.-Y., Baek, K., Ok, Y.S., Park, J.-H., 2015. Stabilization of As-,
337 Pb-, and Cu-contaminated soil using calcined oyster shells and steel slag. *Environ. Sci. Pollut. Res.* 22, 11162-
338 11169.

339 Moon, D.H., Wazne, M., Yoon, I.H., Grubb, D.G., 2008. Assessment of cement kiln dust (CKD) for
340 stabilization/solidification (S/S) of arsenic contaminated soils. *J. Hazard. Mater.* 159, 512-518.

341 Moulin, I., Stone, W.E.E., Sanz, J., Bottero, J.-Y., Mosnier, F., Haehnel, C., 1999. Lead and zinc retention during
342 hydration of tri-calcium silicate: a study by sorption isotherms and ²⁹Si nuclear magnetic resonance
343 spectroscopy. *Langmuir* 15, 2829-2835.

344 Park, H.-Y. 2003. Development of industrialization technology with starfish. *Food Ind. Nutr.* 8(3), 18-22.

345 Rose, J., Moulin, I., Hazemann, J.-L., Masion, A., Bertsch, P.M., Bottero, J.-Y., Mosnier, F., Haehnel, C., 2000.
346 X-ray absorption spectroscopy study of immobilization processes for heavy metals in calcium silicate hydrates:
347 1. case of lead. *Langmuir* 16, 9900-9906.

348 Rose, J., Moulin, I., Mason, A., Bertsch, P.M., Wiesner, M.R., Bottero, J.-Y., Mosnier, F., Haehnel, C., 2001. X-
349 ray absorption spectroscopy study of immobilization processes for heavy metals in calcium silicate hydrates.
350 2. Zinc. *Langmuir* 17, 3658-3665.

351 Ruiz, M.C., Irabien, A., 2004. Environmental behavior of cement-based stabilized foundry sludge products
352 incorporating additives. *J. Hazard. Mater.* B109, 45-52.

353 Tessier, A., Campbell, P.G.C., Bisson, M., 1979. Sequential extraction procedure for speciation of particulate trace
354 metals. *Anal. Chem.* 51, 844-851.

355 USEPA, 1999. Land disposal restrictions phase II-universal treatment standards, and treatment standards for
356 organic toxicity characteristics wastes and newly listed wastes, final rule, Title 40 Code Fed. Regul. (CFR), 7-
357 1-99 Edition, Part 268, (Chapter I).

358 USEPA, 1992. Test Methods for Evaluating Solid Waste, Physical/Chemical Methods, SW-846, third ed., Method
359 1311, USEPA, Washington D.C.

360 Wang, S.Y., Vipulanandan, C., 1996. Leachability of lead from solidified cement-fly ash binders. Cement
361 Concrete Res. 26(6), 895-905.
362

363 **Table 1** Physicochemical and mineralogical properties and total concentrations of heavy metals in the soil.

Soil properties	Contaminated Soil	Korean warning standards ^a
Soil pH	7.22	
Organic matter content (%) ^b	3.16	
Composition (%) ^c		
Sand	66.3	
Silt	13.5	
Clay	20.2	
Texture ^d	Sandy loam	
Heavy metals (mg·kg ⁻¹)		
Pb	980	200
Zn	890	300
Mineral compositions ^e	Quartz Albite Muscovite	

364 ^aKorean warning standards for soils in residential areas.

365 ^bOrganic matter content (%) was calculated from measured loss-on-ignition (LOI) (Ball 1964; FitzPatrick 1983).

366 ^cSoil classification was conducted using a particle size analyzer (PSA); Sand, 20-2,000 μm; silt, 2-20 μm; clay,
367 <2 μm.

368 ^dSoil texture as suggested by the United States Department of Agriculture (USDA).

369 ^eMineral compositions were obtained using the Jade software (MDI 2005).

370

371

372

373

374

375

376

377

378

379

380

381

382

383 **Table 2** Major chemical composition of contaminated soil and starfish (wt.%).

	Contaminated soil	NSF	CSF
Chemical composition (wt.%)			
SiO ₂	71.3	4.87	4.63
Al ₂ O ₃	15.8	1.51	1.07
Fe ₂ O ₃	3.34	0.39	0.50
K ₂ O	3.19	1.57	1.46
CaO	1.07	38.7	70.7
MgO	0.92	2.30	9.25
TiO ₂	0.51	0.05	0.03
P ₂ O ₅	0.20	1.13	1.21
pH (1:5)	7.22	7.14	12.52
LOI	3.16	39.9	0.87

384

385

386

387

388

389

390

391

392

393

394

395

396

397

398

399

400

401

402

403

404

405 **Table 3** Treatability matrix for Pb and Zn contaminated soil.

Sample ID	Contaminated soil (100 wt%)	NSF (wt%)	CSF (wt%)	L:S ratio (l kg ⁻¹)
Control	√	0	-	20:1
2% NSF	√	2	-	20:1
4% NSF	√	4	-	20:1
6% NSF	√	6	-	20:1
8% NSF	√	8	-	20:1
10% NSF	√	10	-	20:1
1% CSF	√	-	1	20:1
2% CSF	√	-	2	20:1
3% CSF	√	-	3	20:1
4% CSF	√	-	4	20:1
5% CSF	√	-	5	20:1

406

407

408

409

410

411

412

413

414

415

416

417

418

419

420

421

422

423

424

425

426

427 **Fig. 1.** XRPD patterns for NSF and CSF.

428 **Fig. 2.** (a) TCLP Pb and (b) TCLP Zn results for NSF treated samples; curing period 28 days.

429 **Fig. 3.** (a) TCLP Pb and (b) TCLP Zn results for CSF treated samples; curing period 28 days.

430 **Fig. 4.** Chemical fractions of Pb and Zn for (a) the control and 10 wt.% NSF treated samples and (b) the control

431 and 5 wt.% CSF treated samples.

432 **Fig. 5.** SEM-EDX analyses and element dot maps for (a) Pb and (b) Zn in contaminated soil treated with 5

433 wt.% CSF.

434

435

436

437

438

439

440

441

442

443

444

445

446

447

448

449

450

451

452

453

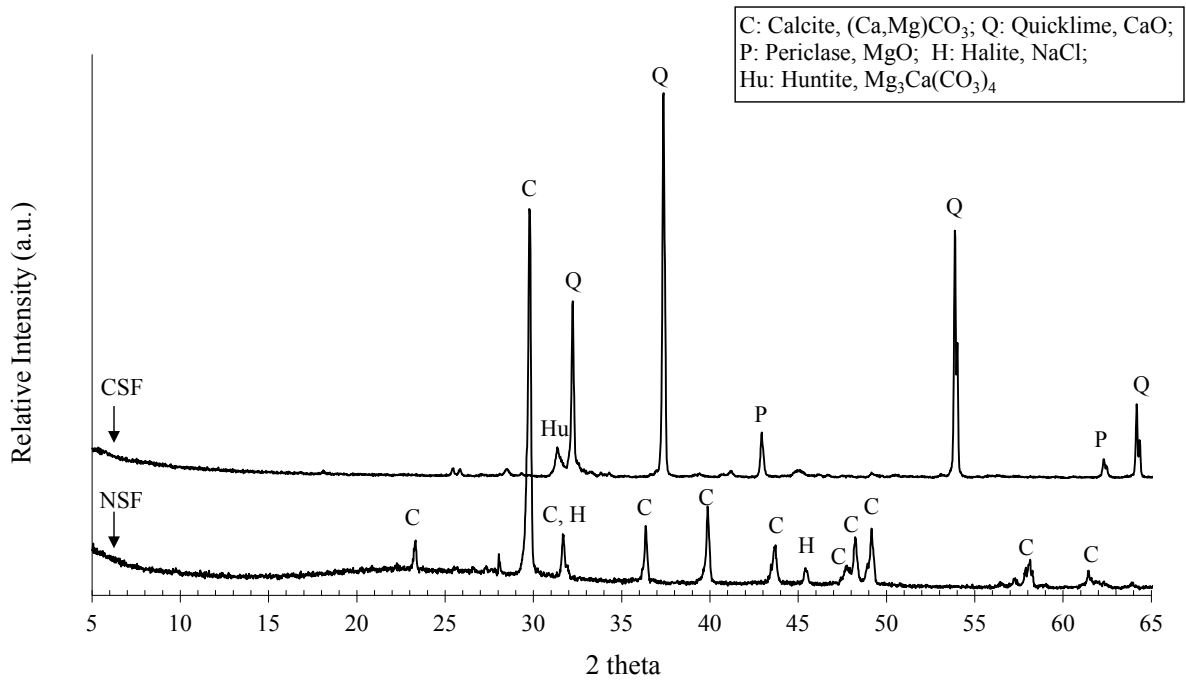
454

455

456

457 Fig. 1.

458



459

460

461

462

463

464

465

466

467

468

469

470

471

472

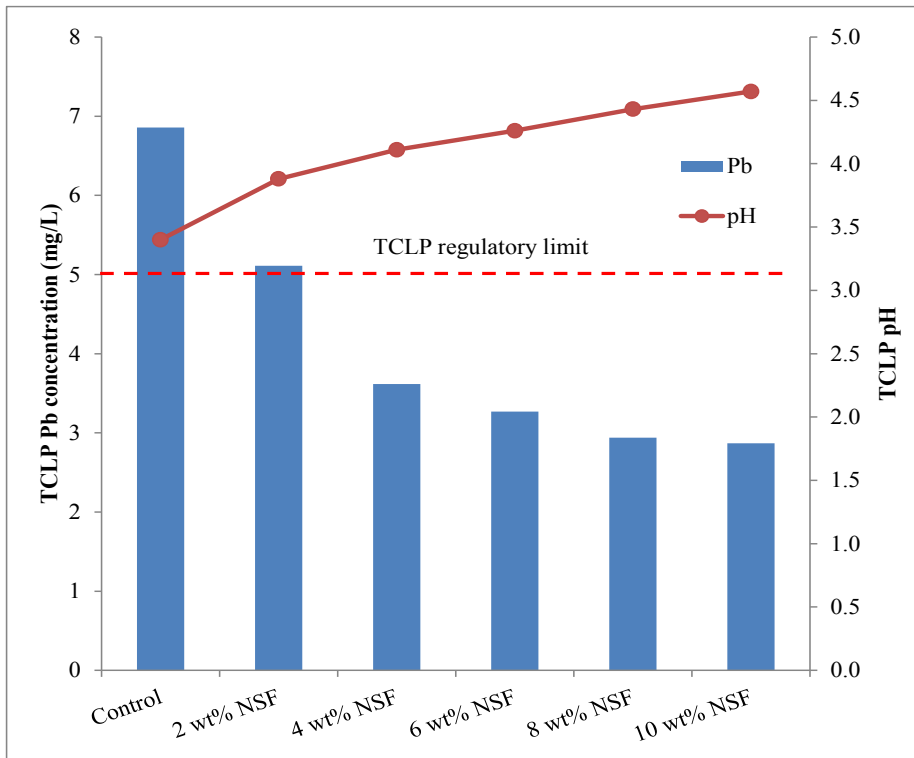
473

474

475

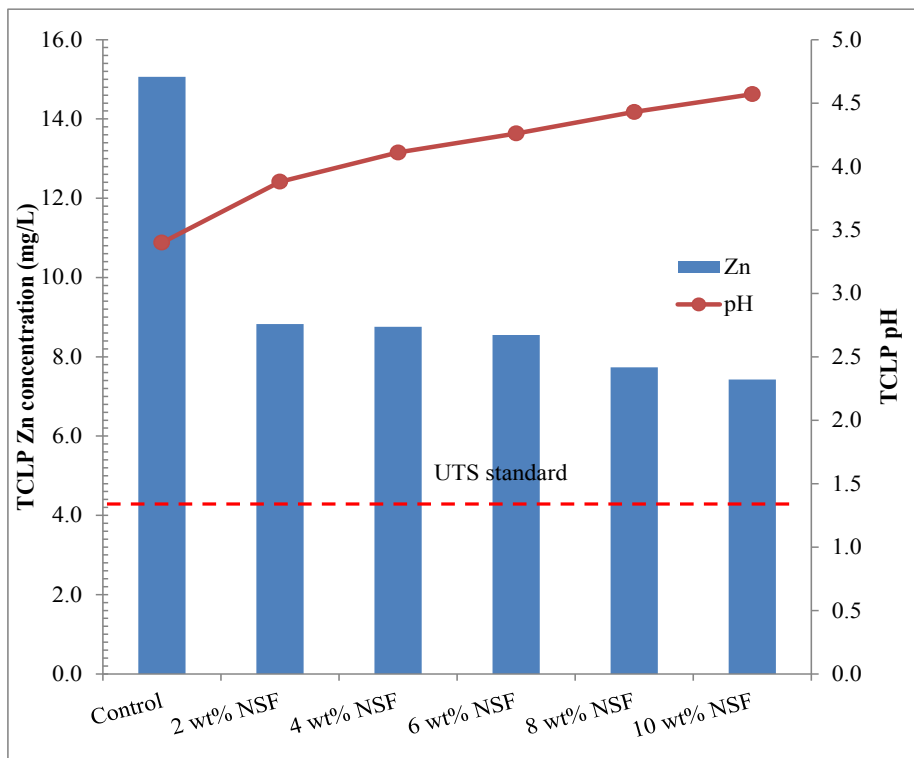
476 Fig. 2.

477 (a)



478

479 (b)



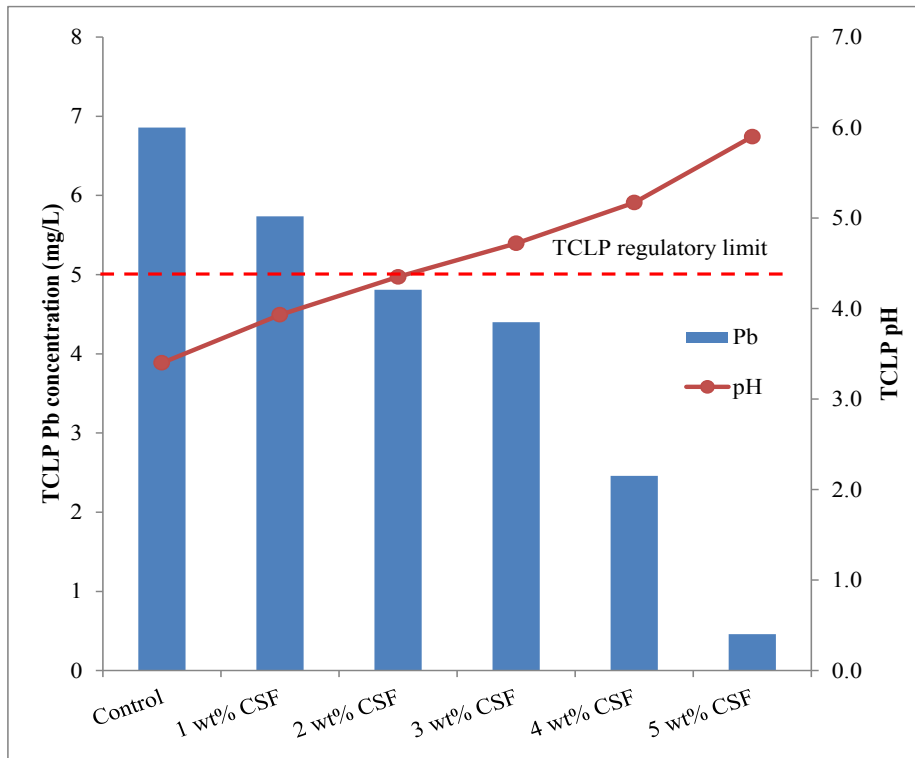
480

481

482

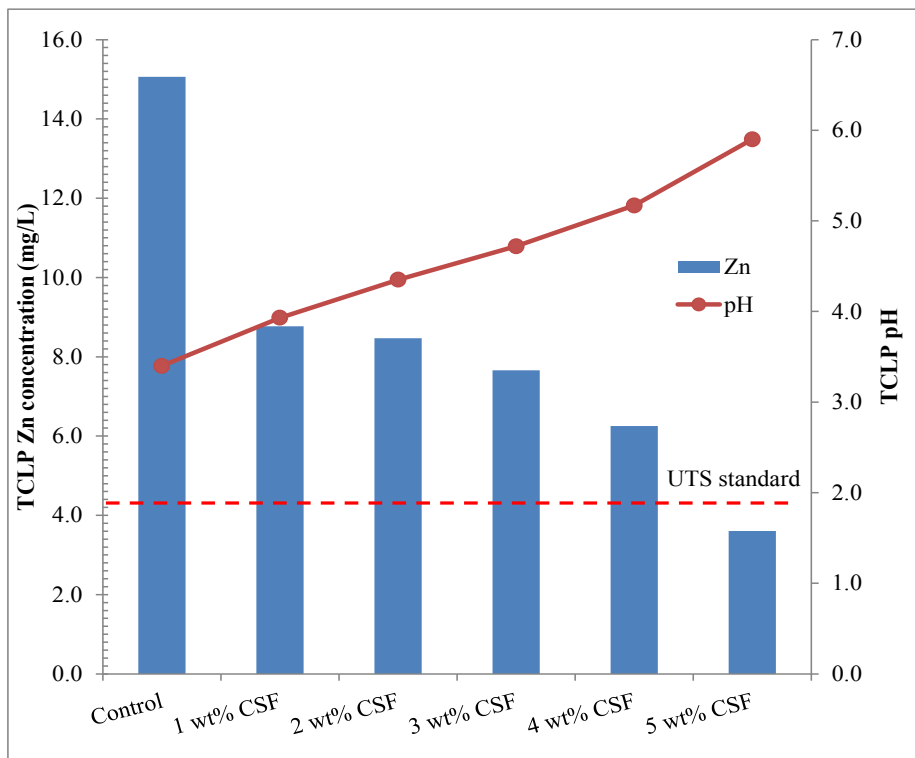
483 Fig. 3.

484 (a)



485

486 (b)



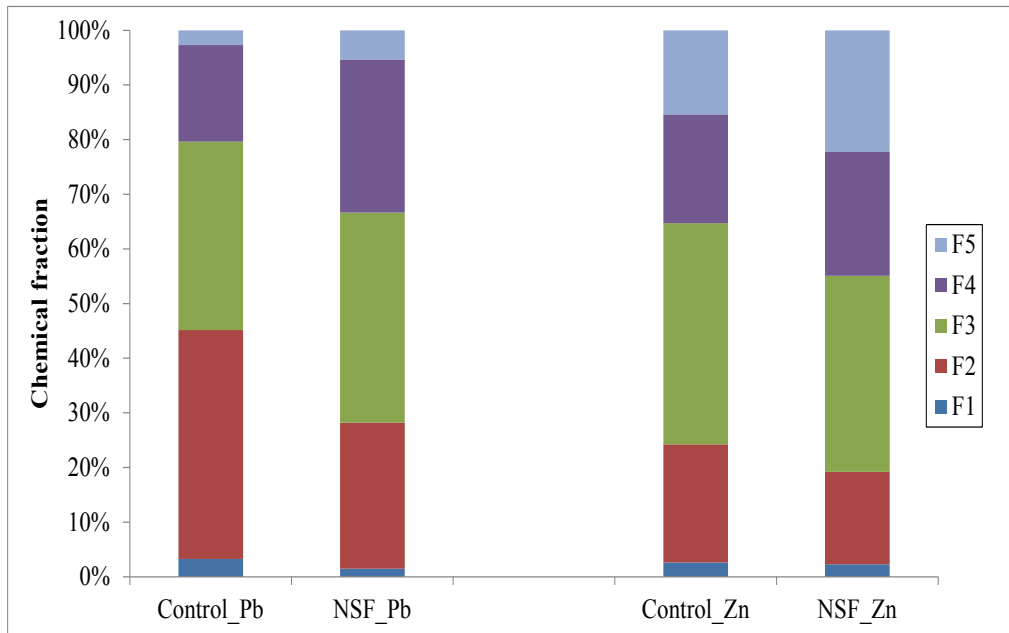
487

488

489

490 Fig. 4.

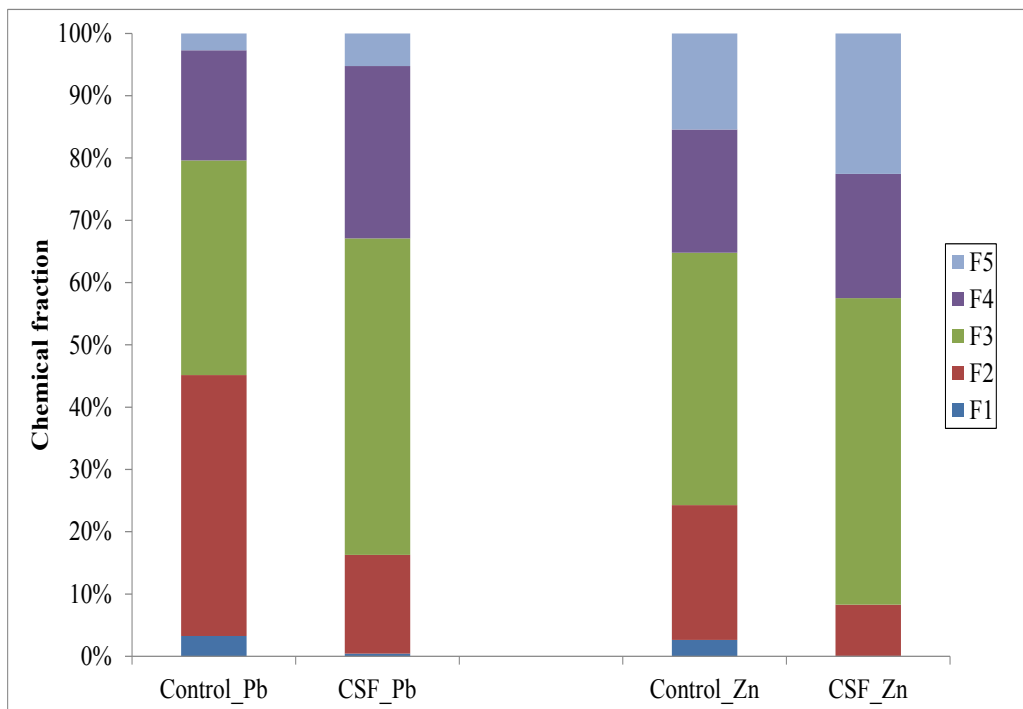
491 (a)



492

493

494 (b)



495

496

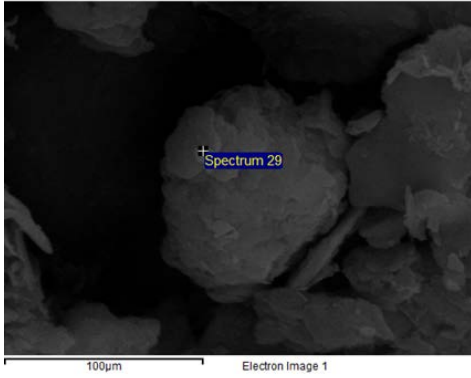
497

498

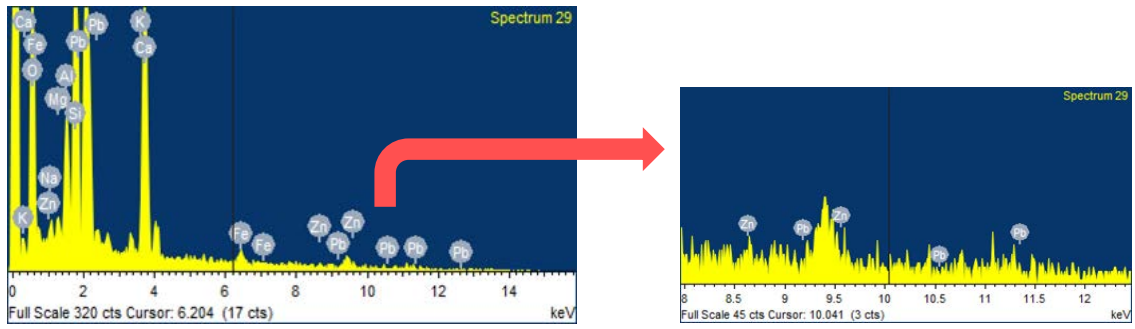
499

500 Fig. 5.

501 (a)

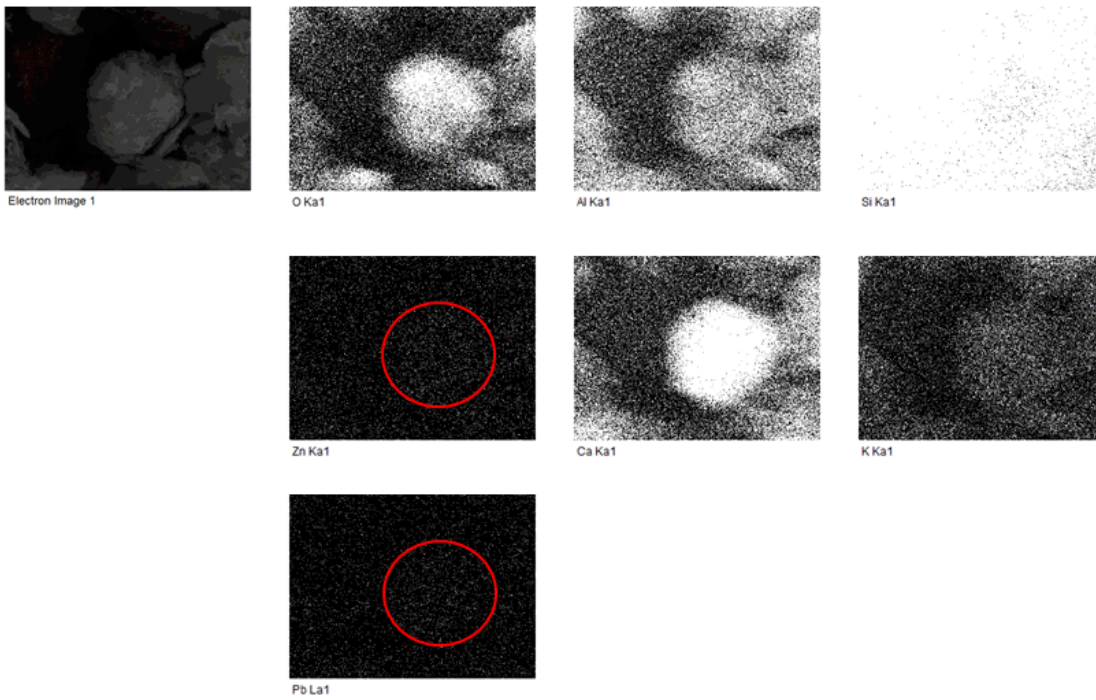


502



503

504 (b)



505